NANOSYSTEMS:
PHYSICS, CHEMISTRY, MATHEMATICS

Dymova A.L., et al. *Nanosystems: Phys. Chem. Math.*, 2024, **15** (4), 481–486.
http://nanojournal.ifmo.ru
DOI 10.17586/2220-8054-2024-15-4-481-486

Original article

Crystalline $LiYF_4$:Nd^{3+} nanoparticles synthesized via laser ablation method in water solutions of ethanol

Anna L. Dymova[1,a], Vadim A. Prikazchikov[1], Anna V. Astrakhantseva[1], Timur M. Minnebaev[1], Mintimir R. Zaitov[1], Maksim S. Pudovkin[1], Alexey S. Nizamutdinov[1,b]

[1]Kazan Federal University, Kazan, Russian Federation

[a]anyuta_dymova@mail.ru, [b]anizamutdinov@mail.ru

Corresponding author: Anna L. Dymova, anyuta_dymova@mail.ru

PACS 78.67.Bf, 81.16.-c

ABSTRACT In this work, a set of crystalline $LiYF_4$:Nd^{3+} nanoparticles with an average size of about 35 nm, were successfully synthesized via laser ablation method in liquid (combination of ethanol and water). The samples have trigonal structure corresponding to $LiYF_4$ host. The spectral and kinetic characteristics of the synthesized nanoparticles corresponded to the characteristics of the target $LiYF_4$:Nd^{3+} bulk crystal. In particular, the luminescence decay curves for the $^4F_{3/2} \rightarrow {}^4I_{11/2}$ radiative transition (Nd^{3+}) are single-exponential and the decay times were around 517 μs, which is typical for Nd^{3+} in $LiYF_4$ host. It has been established that the decrease in the power density of laser radiation energy leads to the increase of the average particle size.

KEYWORDS laser ablation, laser ablation in liquids, $LiYF_4$ nanoparticles, Nd^{3+} nanoparticle synthesis

ACKNOWLEDGEMENTS This research was funded by the subsidy allocated to Kazan Federal University for the state assignment in the sphere of scientific activities: FZSM-2023-0012.

FOR CITATION Dymova A.L., Prikazchikov V.A., Astrakhantseva A.V., Minnebaev T.M., Zaitov M.R., Pudovkin M.S., Nizamutdinov A.S. Crystalline $LiYF_4$:Nd^{3+} nanoparticles synthesized via laser ablation method in water solutions of ethanol. *Nanosystems: Phys. Chem. Math.*, 2024, **15** (4), 481–486.

1. Introduction

In the past two decades, one of the most rapidly growing areas of science and industry has been the synthesis of nanoparticles with specified morphology and desirable physicochemical properties. Among many methods for the synthesis of nanomaterials, the laser ablation in liquid plays a special role. Indeed, laser ablation is a relatively simple and time consuming method of the nanoparticle synthesis, which allows obtaining metal nanoparticles [1, 2], nanoparticles of semiconductor compounds [3, 4], as well as dielectric ones (in particular, fluoride and oxide compounds [5, 6]). The laser ablation method in liquid has a number of advantages: firstly, it is a relatively fast method of producing particles that does not require such specialized conditions as high temperature, pressure, and the use of toxic compounds or acids as reaction environment. Secondly, it allows controlling such properties of the resulting nanoparticles as shape, size, and size distribution by varying the laser irradiation parameters (wavelength, frequency and duration of the pulses, power density). The characteristics of the liquid (pH level, chemical composition of the solvent and its polarity) have a notable impact on the above-mentioned characteristics [7–11]. In particular, in [12, 13], it was shown that an increase in the power density of laser irradiation increases the average size of the nanoparticles. Despite a number of advantages, laser ablation in liquid is not widely used as a method of industrial synthesis. The main reason is the low productive capacity of the process compared to chemical methods. There is large dispersion of the resulting nanoparticles in shape and size (width of the size distribution is from approximately 1–5 nm to 100–150 nm) in the case of non-optimal choice of the laser irradiation parameters [7].

This work demonstrates the possibility of the $LiYF_4$:Nd^{3+} nanoparticle synthesis via laser ablation in the liquid using a bulk crystal of a similar composition as a target for laser irradiation. It was previously shown that the laser ablation torch of this crystal, there are all the necessary components for the synthesis of this nanosized compound [14]. The possibility of the synthesizing of the thin films [15] and nanoparticles [16] of this compound by laser ablation was also shown. The main objective of this work is to study the dependence of laser irradiation parameters and liquid parameters on characteristics of $LiYF_4$:Nd^{3+} nanoparticles. The mechanisms explaining the obtained results were suggested [17–21].

The choice of $LiYF_4$ host is based on the fact, that it has low phonon energy resulting in lower probability of non-radiative multiphonon relaxation. It also demonstrates high chemical, mechanical and thermal stability [22–24]. In its turn, Nd^{3+} ion has a unique electron level structure and can be optically excited in the broad spectral range including so-called "biological window". Due to the thermally coupled Stark components of the luminescence peaks nanoparticles doped with Nd^{3+} ions can serve as luminescent thermometers operating in the physiological temperature range. Specifically, Nd^{3+} doped fluoride nanoparticles were successfully utilized for hyperthermia with simultaneous remote optical temperature

sensing for phantom tissue [25]. On the other hand, Nd^{3+} doped SrF_2 nanoparticles demonstrated their efficiency in bioimaging of mouse organs in the biological window (1000–1400 nm) [26].

2. Materials and methods

2.1. Synthesis of $LiYF_4$:Nd^{3+} nanoparticles

The nanoparticles were synthesized using a pulsed Nd:YAG laser (LQ529B) generating 532 nm nanosecond pulse irradiation (pulse duration and pulse repetition rate were 10 ns and 10 Hz, respectively). The target $LiYF_4$:Nd^{3+} (1.0 at.%) bulk crystal was grown by the Bridgman-Stockbarger method. Irradiation was carried out in solution of deionized water with 10% volume fraction of ethanol. The effect of laser energy power density on the nanoparticle size in the water/ethanol = 90/10% solution was also investigated. The chosen power densities were 0.9, 1.1, and 1.5 J/cm^2. Particles were collected from the colloidal solution using a syringe. Next, the nanoparticles were dried in a dustproof chamber in air. The scheme of the experimental set-up is presented in Fig. 1. To record the luminescence spectra, a CCD StellarNet spectrometer was used (1–2 nm resolution and 200–1200 nm spectral range). To record the luminescence decay curves, a combination of an MDR-23 monochromator (resolution 0.1 nm, spectral range 200–2000 nm), a photomultiplier tube (FEU-62) and a Bordo oscilloscope (10 bit, bandwidth 200 MHz) was used.

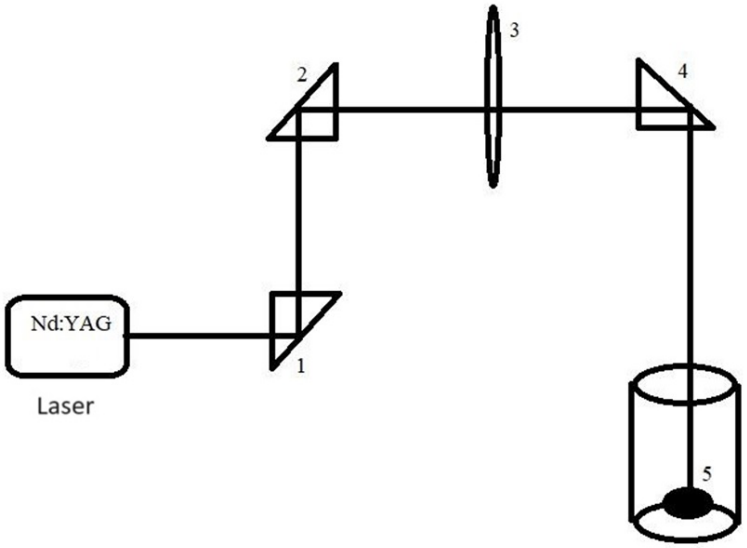

FIG. 1. Experimental set-up for synthesis via laser ablation consisting of a set of prisms (1, 2, and 4), lens (3), and the target (5) in the liquid

2.2. Physicochemical characterization of the samples

The work examined the morphology of nanoparticles, as well as the phase composition. The study of all the samples was carried out in three stages. The phase composition of the samples was studied via X-ray diffraction (XRD) using an MD-10 EFA setup (FeK_α radiation at λ=1.93597 wavelength). The scanning electron microscope EVO 50 XVP Carl Zeiss was used to investigate the morphology and size of the samples.

3. Results and discussion

The XRD pattern of the $LiYF_4$:Nd^{3+} nanoparticles is represented in Fig. 2.

The obtained XRD pattern corresponds to the $LiYF_4$ host. The impurity peaks or double phase as well as the presence of the amorphous phase were not found. The calculated lattice parameters were a= 0.513(6), c= 1.070(7) are typical for the $LiYF_4$ host [20]. SEM image of the nanoparticles synthesized in water/ethanol = 90/10% solution presented in Fig. 3.

It can be seen, that the nanoparticles have predominantly spherical shape. The size distribution histograms of the obtained nanoparticles are presented n Fig. 4.

The mechanism of nanoparticle formation is the crystallization from the gas phase. In particular, under the influence of a laser pulse, the target material is heated and evaporates, forming a drop in a bubble, and then crystallizes as a result of cooling [9, 11–13]. Since the thermal conductivity of water is high, the molten droplets dispersed in solvent will quickly condense to form large sized particles. For solvents having lower thermal conductivity, the initial particles exist longer in the melted condition and fractionize into smaller particles. The ethanol molecules can act as a shell that prevents the aggregation of nanoparticles [18, 19]. It is of interest to consider the influence of laser radiation energy density on the sizes of nanoparticles. Fig. 4 shows graphs of particle size distribution. According to the data obtained, it can be said that

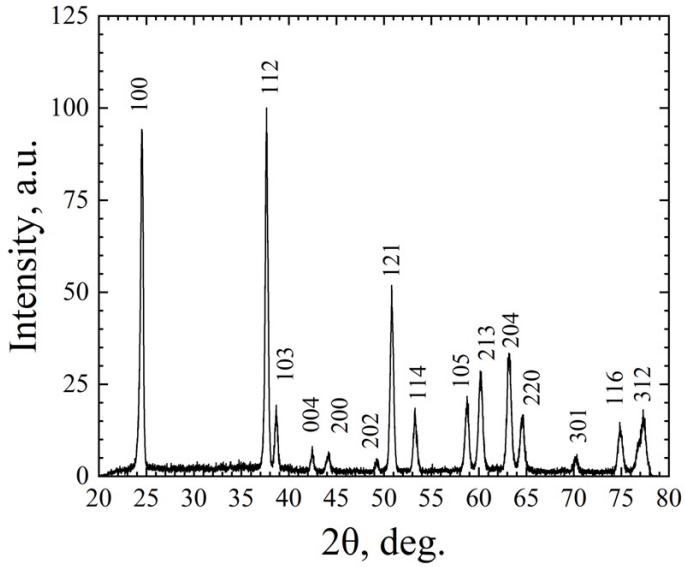

FIG. 2. XRD pattern of the $LiYF_4$:Nd^{3+} nanoparticles

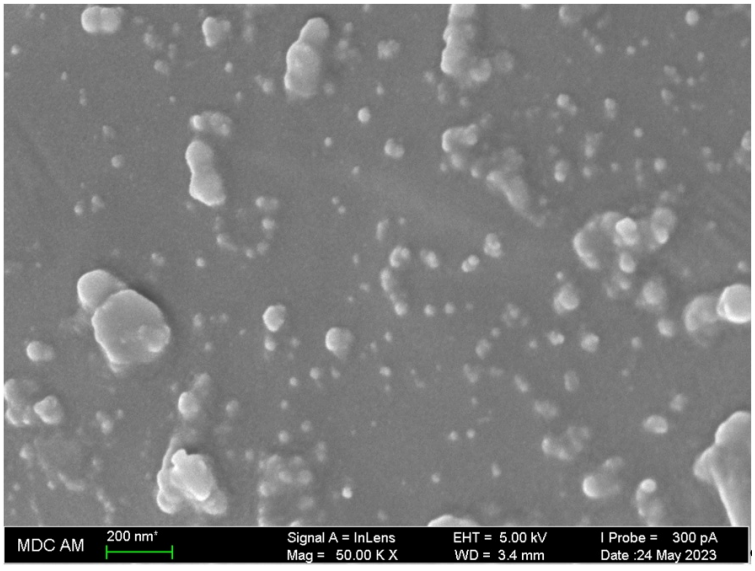

FIG. 3. SEM image of the nanoparticles synthesized in water/ethanol = 90/10% solution obtained for laser radiation energy density 0.9 J/cm^2

with the increase of power density of laser radiation energy, the average particle size increases. This can be related to the fact that higher energy heats up the nanoparticles more efficiently, which leads to their aggregation and fusing into one crystalline agglomerate [20, 21].

Optical excitation of nanoparticles was carried out by laser irradiation at 790 nm wavelength ($^4I_{9/2}$–$^4F_{5/2}$ absorption band of Nd^{3+} ions). Fig. 5a shows the luminescence spectrum of $LiYF_4$:Nd^{3+} nanoparticles recorded at room temperature. The spectrum contains luminescence bands corresponding to the $^4F_{3/2} \rightarrow ^4I_{9/2}$ (849–950 nm) and $^4F_{3/2} \rightarrow ^4I_{11/2}$ 1039–1080 nm) radiative transitions of Nd^{3+} ions [15, 22].

Fig. 5b demonstrates the luminescence decay curve at 1046 nm ($^4F_{3/2} \rightarrow ^4I_{11/2}$ radiative transition of Nd^{3+} ions) upon excitation at 790 nm. The curve has a single-exponential dependence with a calculated decay around 517 μs, which is typical for $LiYF_4$:Nd^{3+} phosphors [15]. In addition, the single-exponential nature of the luminescence decay suggests that Nd^{3+} ions are distributed homogeneously in the nanoparticles and do not form clusters. In particular, during clustering, Nd^{3+} ions interact more effectively with each other in clusters, which can lead to enhanced quenching of the $^4F_{3/2}$ state due to concentration quenching and/or cross-relaxation. This can lead to the appearance of a short-lived component in the kinetics of luminescence decay [22].

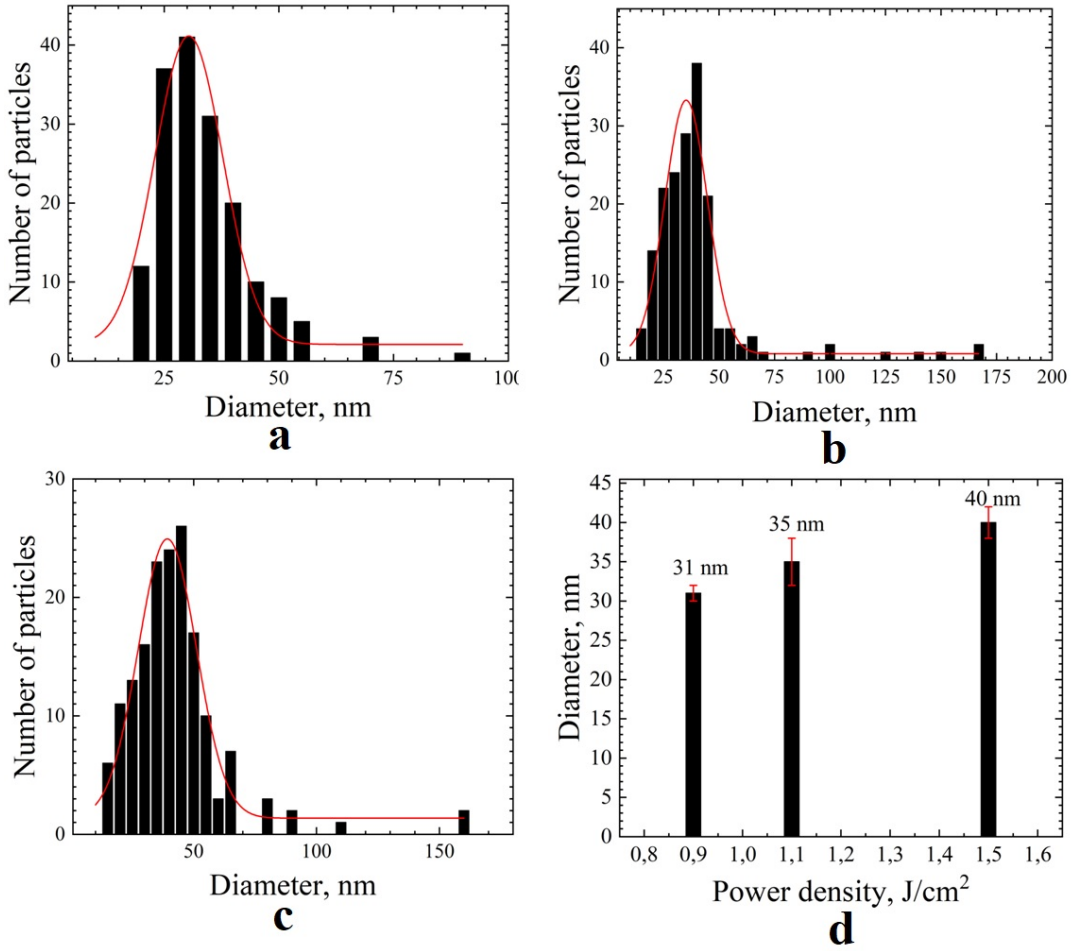

FIG. 4. The nanoparticle size distribution obtained for laser radiation energy density a) 0.9, b) 1.1, c) 1.5 J/cm^2; d) The nanoparticle size dependence on the energy density of laser radiation

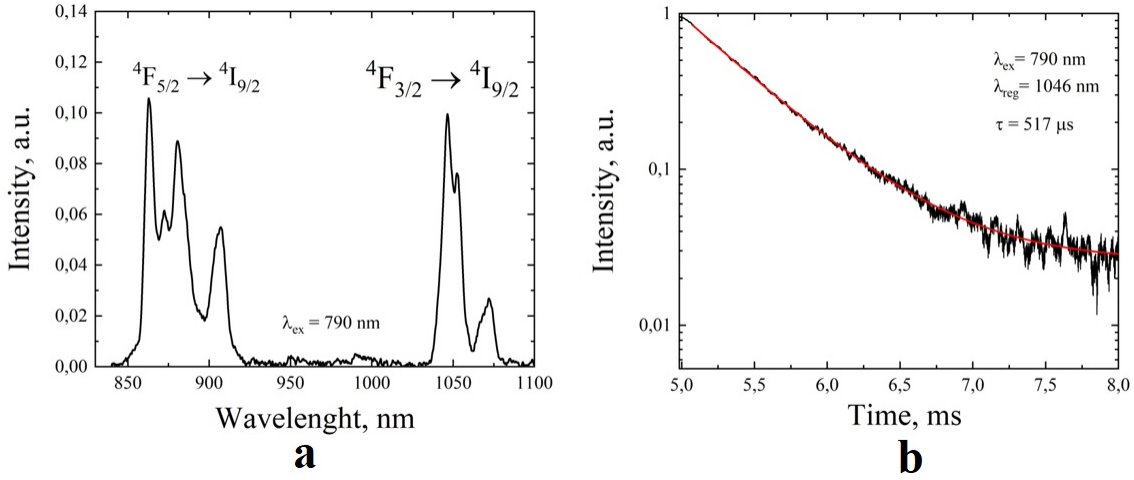

FIG. 5. Room temperature luminescence spectrum of $LiYF_4:Nd^{3+}$ nanoparticles (a) and luminescence decay kinetic at the registration wavelength λ=1046 nm (b) for a sample synthesized from a solution with a volume fraction of ethanol 10%, excitation wavelength λ=790 nm

4. Conclusions

Nanoparticles of $LiYF_4$:Nd^{3+} were successfully synthesized by laser ablation in liquid. Specifically, the laser irradiation was carried out in solutions of deionized water with volume fractions of ethanol in solution of 10%. The effect of laser energy power density on the nanoparticle size in the water/ethanol = 90/10% solution was also investigated. The chosen power densities were 0.9, 1.1, and 1.5 J/cm^2. The resulting samples had a trigonal structure corresponding to the $LiYF_4$ host. The nanoparticles synthesized in aqueous solutions with ethanol, have the average particle size around 72 nm. The hypothesis explaining the observed results was made. Specifically, the thermal conductivity of water is high, the molten droplets dispersed in solvent will quickly condense to form large sized particles. For solvents having higher thermal conductivity, the initial particles exist longer in the melted condition and fractionize into smaller particles. The ethanol molecules can act as a shell that prevents the aggregation of nanoparticles. It is also shown, that with the increase of the power density of laser radiation energy, the average particle size increases. This can be related to the fact that higher energy heats up the nanoparticles more efficiently, which leads to their aggregation and fusing into one crystalline agglomerate. The spectral and kinetic characteristics of the synthesized nanoparticles also corresponded to the target bulk crystal. In particular, upon 790 nm excitation, a characteristic luminescence spectrum was observed for the $^4F_{3/2} \rightarrow {}^4I_{9/2}$ (849–950 nm) and $^4F_{3/2} \rightarrow {}^4I_{11/2}$ 1039–1080 nm) radiative transitions of Nd^{3+} ions. The curve has a single-exponential dependence with a calculated decay around 517 μs, which is typical for $LiYF_4$:Nd^{3+} phosphors.

References

[1] Compagnini G., Scalisi A.A., Puglisi O. Production of gold nanoparticles by laser ablation in liquid alkanes. *Journal of Applied Physics*, 2003, **94**(12), P. 7874–7877.

[2] Lau Truong S., Levi G., Bozon-Verduraz F., Petrovskaya A.V., Simakin A.V., Shafeev G.A. Generation of Ag nanospikes via laser ablation in liquid environment and their activity in SERS of organic molecules. *Applied Physics A*, 2007, **89**, P. 373–376.

[3] Sajti C.L., Giorgio S., Khodorkovsky V., Marine W. Femtosecond laser synthesized nanohybrid materials for bioapplications. *Applied Surface Science*, 2007, **253**(19), P. 8111–8114.

[4] Usui H., Shimizu Y., Sasaki T., Koshizaki N. Photoluminescence of ZnO nanoparticles prepared by laser ablation in different surfactant solutions. *The Journal of Physical Chemistry B*, 2005, **109**(1), P. 120–124.

[5] Amans D., Malaterre C., Diouf M., Mancini C., Chaput F., Ledoux G., Perriat P. Synthesis of oxide nanoparticles by pulsed laser ablation in liquids containing a complexing molecule: impact on size distributions and prepared phases. *The Journal of Physical Chemistry C*, 2011, **115**(12), P. 5131–5139.

[6] Ledoux G., Amans D., Dujardin C., Masenelli-Varlot K. Facile and rapid synthesis of highly luminescent nanoparticles via pulsed laser ablation in liquid. *Nanotechnology*, 2009, **20**(44), P. 445605.

[7] Makarov G.N. Laser applications in nanotechnology: nanofabrication using laser ablation and laser nanolithography. *Physics-Uspekhi*, 2013, **56**(7), P. 643.

[8] Buesser B., Groehn A.J. Multiscale Aspects of Modeling Gas Phase Nanoparticle Synthesis. *Chemical Engineering & Technology*, 2012, **35**(7), P. 1133–1143.

[9] Naser H., Alghoul M.A., Hossain M.K., Asim N., Abdullah M.F., Ali M.S., Amin N. The role of laser ablation technique parameters in synthesis of nanoparticles from different target types. *Journal of Nanoparticle Research*, 2019, **21**, P. 1–28.

[10] Wang Y.L., Xu W., Zhou Y., Chu L.Z., Fu G.S. Influence of pulse repetition rate on the average size of silicon nanoparticles deposited by laser ablation. *Laser and Particle Beams*, 2007, **25**(1), P. 9–13.

[11] Al-Azawi M.A., Bidin N., Bououdina M., Abbas K.N., Al-Asedy H. J., Ahmed O.H., Thahe A.A. The effects of the ambient liquid medium on the ablation efficiency, size and stability of silver nanoparticles prepared by pulse laser ablation in liquid technique. *J. Teknol*, 2016, **78**(3), P. 7–11.

[12] Pereira H., Moura C.G., Miranda G., Silva F.S. Influence of liquid media and laser energy on the production of MgO nanoparticles by laser ablation. *Optics & Laser Technology*, 2021, **142**, P. 107181.

[13] Wang H., Odawara O., Wada H. Facile and chemically pure preparation of YVO_4:Eu^{3+} colloid with novel nanostructure via laser ablation in water. *Scientific Reports*, 2016, **6**(1), P. 20507.

[14] Barsanti S., Favilla E., Bicchi P. Emission and electron/ion analysis of the ablated plume from $LiYF_4$ crystals doped with Tm^{3+} or Nd^{3+} ions. *Radiation Physics and Chemistry*, 2007, **76**(3), P. 512–515.

[15] Barsanti S., Cornacchia F., Di Lieto A., Toncelli A., Tonelli M., Bicchi P. Nd^{3+}-doped fluoride film grown on $LiYF_4$ substrate by pulsed laser deposition. *Thin Solid Films*, 2008, **516**(8), P. 2009–2013.

[16] Lukinova E., Farukhshin I., Nizamutdinov A., Madirov E., Semashko V., Pudovkin M. Ce^{3+} doped $LiYF_4$ nanoparticles fabrication by laser ablation. In EPJ Web of Conferences, 2017, **161**, P. 03014.

[17] Rawat R., Tiwari A., Arun N., Rao S.N., Pathak A.P., Tripathi A. Solvents effect on the morphology and stability of Cu/CuO nanoparticles synthesized at high fluence laser ablation. *ChemistrySelect*, 2019, **4**(35), P. 10471–10482.

[18] Naderi-Samani H., Razavi R.S., Mozaffarinia R. Investigating the effect of 532 nm and 1064 nm wavelengths and different liquid media on the qualities of silver nanoparticles yielded through laser ablation. *Materials Chemistry and Physics*, 2023, **305**, P. 128001.

[19] Goncharova D.A., Kharlamova T.S., Reutova O.A., Svetlichnyi V.A. Water–ethanol CuOx nanoparticle colloids prepared by laser ablation: Colloid stability and catalytic properties in nitrophenol hydrogenation. *Colloids and Surfaces A: Physicochemical and Engineering Aspects*, 2021, **613**, P. 126115.

[20] Thoma R.E., Brunton G.D., Penneman R.A., Keenan T.K. Equilibrium relations and crystal structure of lithium fluorolanthanate phases. *Inorganic Chemistry*, 1970, **9**(5), P. 1096–1101.

[21] Alakshin E.M., Kondratyeva E.I., Nuzhina D.S., Iakovleva M.F., Kuzmin V.V., Safiullin K.R., Tagirov M.S. The self-assembly of DyF_3 nanoparticles synthesized by chloride-based route. *Journal of Nanoparticle Research*, 2018, **20**, P. 1–11.

[22] Pudovkin M.S., Ginkel A.K., Morozov O.A., Kiiamov A.G., Kuznetsov M.D. Highly-sensitive lifetime optical thermometers based on Nd^{3+}, Yb^{3+}:YF_3 phosphors. *Journal of Luminescence*, 2022, **249**, P. 119037.

[23] Anbharasi L., Rekha E.B., Rahul V.R., Roy B., Gunaseelan M., Yamini S., Senthilselvan J. Tunable emission and optical trapping of upconverting $LiYF_4$: Yb, Er nanocrystal. *Optics & Laser Technology*, 2020, **126**, P. 106109.

[24] Fedorov P.P., Semashko V.V., Korableva S.L. Lithium rare-earth fluorides as photonic materials: 1. Physicochemical characterization. *Inorganic Materials*, 2022. **58**(3), P. 223–245.

[25] Ximendes E.C., Rocha U., Kumar K.U., Jacinto C., Jaque D. LaF_3 core/shell nanoparticles for subcutaneous heating and thermal sensing in the second biological-window. *Applied Physics Letters*, 2016, **108**(25).

[26] Villa I., Vedda A., Cantarelli I.X., Pedroni M., Piccinelli F., Bettinelli M., Garcna D.J. 1.3 μm emitting SrF_2:Nd^{3+} nanoparticles for high contrast in vivo imaging in the second biological window. *Nano Research*, 2015, *8*, P. 649–665.

Submitted 3 December 2023; revised 18 July 2024; accepted 19 July 2024

Information about the authors:

Anna L. Dymova – Kazan Federal University, 18 Kremlyovskaya str, Kazan, 420008, Russian Federation; anyuta_dymova@mail.ru

Vadim A. Prikazchikov – Kazan Federal University, 18 Kremlyovskaya str, Kazan, 420008, Russian Federation

Anna V. Astrakhantseva – Kazan Federal University, 18 Kremlyovskaya str, Kazan, 420008, Russian Federation; ORCID 0000-0002-1670-3064

Timur M. Minnebaev – Kazan Federal University, 18 Kremlyovskaya str, Kazan, 420008, Russian Federation

Mintimir R. Zaitov – Kazan Federal University, 18 Kremlyovskaya str, Kazan, 420008, Russian Federation; ORCID 0009-0003-3621-0982

Maksim S. Pudovkin – Kazan Federal University, 18 Kremlyovskaya str, Kazan, 420008, Russian Federation; ORCID 0000-0002-7455-9611

Alexey S. Nizamutdinov – Kazan Federal University, 18 Kremlyovskaya str, Kazan, 420008, Russian Federation; ORCID 0000-0003-1559-6671; anizamutdinov@mail.ru

Conflict of interest: the authors declare no conflict of interest.